

Supproting infromation

Polar Rotor for Designing Antiferroelectricity-Antiferromagneticty in a Quasi-2D Organic-Inorganic Hybrid Perovskite

Zi-Ao Qiu,^a Hua-Kai Li,^a Ze-Jiang Xu,^a Liang-Han Shen,^a Xiang Zhang,^a Chao Shi,^a Na Wang,^a Xiao-Bin Fu,^b Nian-Tao Yao,^c Heng-Yun Ye,^a and Le-Ping Miao^{*a}

^a Chaotic Matter Science Research Center, International Institute for Innovation, Jiangxi University of Science and Technology, Ganzhou 341000, P.R. China.

^b National Key Laboratory of Thorium Energy, Shanghai Institute of Applied Physics, Chinese Academy of Science, Shanghai, 201800, China.

^c National Key Laboratory of Thorium Energy, Shanghai Institute of Applied Physics, Chinese Academy of Science, Shanghai, 201800, China.

E-mail: L.P.M. (miaoleping@jxust.edu.cn)

Supplementary Index

Note

Calculations of ΔS and N for compound DFCBC and DFCBZ.

Experimental

Sample preparation

General Measurements

X-ray diffraction experiments

Supplemental Figures

Figure S1. The macroscopic shape of the single crystal of crystal (a) DFCBC and (b) DFCBZ.

Figure S2. PXRD patterns of compound (a) DFCBC and (b) DFCBZ.

Figure S3. The thermogravimetric (TG) curve of compound (a) DFCBC and (b) DFCBZ.

Figure S4. (a) DSC curves of CBC at 285–325 K.(b) DSC curves of CBZ at 240–320 K.

Figure S5. Perovskite structure of DFCBZ at LTP and HTP.

Figure S6. Comparison of simulated and experimental variable-temperature PXRD patterns of DFCBC.

Figure S7. Zn–Cl bond length and Cl–Zn–Cl bond angle in DFCBZ in (a) LTP and (b) HTP.

Figure S8. ϵ' and curves of the heating and cooling cycles of (a) DFCBC and (b)DFCBZ at different frequencies.

Figure S9. (a) Temperature dependence of P – E hysteresis loops of DFCBZ at 50 Hz. (b) Schematic diagram for the calculation of energy storage properties of antiferroelectric materials at 333 K.

Figure S10. Temperature-dependent susceptibilities under a dc field of 1 kOe and Curie–Weiss fitted curves for DFCBC.

Supplemental Tables

Table S1. Crystal Data and Structure Refinement Details for DFCBC and CBC.

Table S2. Crystal Data and Structure Refinement Details for DFCBZ and CBZ.

Table S3. Selected bond lengths [\AA] for DFCBC at 300 and 383 K.

Table S4. Selected bond lengths [\AA] for DFCBZ at 300 and 373 K.

Table S5. Bond lengths [\AA] of the hydrogen bond at 300 K of DFCBC.

Table S6. Bond lengths [\AA] of the hydrogen bond at 383 K of DFCBC.

Table S7. Bond lengths [\AA] of the hydrogen bond at 300 K of DFCBZ.

Table S8. Bond lengths [\AA] of the hydrogen bond at 373 K of DFCBZ.

Note

Calculations of ΔS and N for compound DFCBC (Note S1) and DFCBZ (Note S2).

Compound DFCBC

ΔS

$$= \int_{T_1}^{T_2} \frac{Q}{T} dT \approx \frac{\Delta H}{T_c} = \frac{3.164 J \cdot g^{-1} \times 833.91 g \cdot mol^{-1}}{358.55 K} = \frac{2638.49 J \cdot mol^{-1}}{358.55 K} \approx 7.36$$

$$\Delta S = R \ln N$$

$$N = \exp\left(\frac{\Delta S}{R}\right) = \exp\left(\frac{7.36 J \cdot mol^{-1} \cdot K^{-1}}{8.314 J \cdot mol^{-1} \cdot K^{-1}}\right) = 2.42$$

Compound DFCBZ

ΔS

$$= \int_{T_1}^{T_2} \frac{Q}{T} dT \approx \frac{\Delta H}{T_c} = \frac{3.841 J \cdot g^{-1} \times 846.79 g \cdot mol^{-1}}{373 K} = \frac{3252.52 J \cdot mol^{-1}}{373 K} \approx 8.72$$

$$\Delta S = R \ln N$$

$$N = \exp\left(\frac{\Delta S}{R}\right) = \exp\left(\frac{8.72 J \cdot mol^{-1} \cdot K^{-1}}{8.314 J \cdot mol^{-1} \cdot K^{-1}}\right) = 2.85$$

Experimental

Sample preparation:

Materials: $C_4H_7F_2N \cdot HCl$ ($\geq 99\%$, Shanghai Shanghai Titan Technology Co., Ltd.). $C_4H_{10}ClN$ ($\geq 98\%$, Shanghai Shanghai Titan Technology Co., Ltd.). $CoCl_2$ ($\geq 98\%$, Shanghai Titan Technology Co., Ltd.). $ZnCl_2$ ($\geq 98\%$, Shanghai Shanghai Titan Technology Co., Ltd.). HCl (36% ~ 38%, Jiangxi Xinguang Electronic Technology Co., Ltd.). All chemicals are commercially available and used directly without purification.

Synthesis of compound DFCBC: $C_4H_7F_2N \cdot HCl$ has a 2:1 stoichiometric ratio to cobalt chloride. The HCl (36% ~ 38%) solution as the solvent and slowly evaporated on a constant temperature heating table at 313 K. After about three days, DFCBC crystals containing precipitated crystals were obtained.

Synthesis of compound DFCBZ: $C_4H_7F_2N \cdot HCl$ Hydrochloride has a 2:1 stoichiometric ratio to zinc chloride. The HCl (36% ~ 38%) solution as the solvent and slowly evaporated on a constant temperature heating table at 313 K. After about three days, DFCBZ crystals containing precipitated crystals were obtained.

Synthesis of compound CBC: $C_4H_{10}ClN$ has a 2:1 stoichiometric ratio to cobalt chloride. The HCl (36% ~ 38%) solution as the solvent and slowly evaporated on a constant temperature heating table at 313 K. After about two days, DFCBZ crystals containing precipitated crystals were obtained.

Synthesis of compound CBZ: $C_4H_{10}ClN$ has a 2:1 stoichiometric ratio to zinc chloride. The HCl (36% ~ 38%) solution as the solvent and slowly evaporated on a constant temperature heating table at 313 K. After about two days, DFCBZ crystals containing precipitated crystals were obtained.

General measurements:

The Powder X-ray Diffraction (PXRD) were measured at a measurement angle of 5° – 50° and a scan rate of $5^\circ/\text{min}$ on Rigaku D/MAX 2000 PC X-ray diffractometer. And the X-ray wavelength is 0.15406 nm.

Thermogravimetric (TG) was measured on a NETZSCH STA2500 instrument under a nitrogen atmosphere with a heating rate of 10 K/min.

Differential scanning calorimetry (DSC) tests were performed in a nitrogen atmosphere using a DSC 214 Polyma instrument at a heating/cooling rate of 10 K/min.

Dielectric measurement: For dielectric measurements, the powder samples were used as the plate with a thickness of around 0.5 mm and an area of around 5 mm^2 . Carbon conducting paste deposited on the plate surfaces was used as electrodes. A Tonghui TH2828A impedance analyzer was used to measure the dielectric constants.

The variable temperature P – E hysteresis loops of DFCBC were performed on the thin crystal ($0.5160 \text{ mm} \times 0.106 \text{ mm}$) through a Radiant Precision Premier II instrument was used to measure.

Magnetic measurements were performed with a Quantum Design SQUID magnetometer (MPMSXL-7) magnetometer. The diamagnetic contribution calculated from Pascal constants was corrected in the data.

X-ray diffraction experiments:

Single-crystal X-ray diffraction studies were recorded on a Rigaku synergy diffractometer using the ω scan technique with Mo-K α ($\lambda = 0.71073 \text{ \AA}$) radiation. All structures are solved using direct methods and refined using the full matrix least squares technique in the SHELX2016 package. At high-temperature phase, the space groups were chosen according to the Aizu principle. The organic cations were not modeled according to its chemical sense, because of the highly disordered form at high-temperature phase. Detailed crystallographic data are recorded in Tables S1–S8.

Supplemental Figures

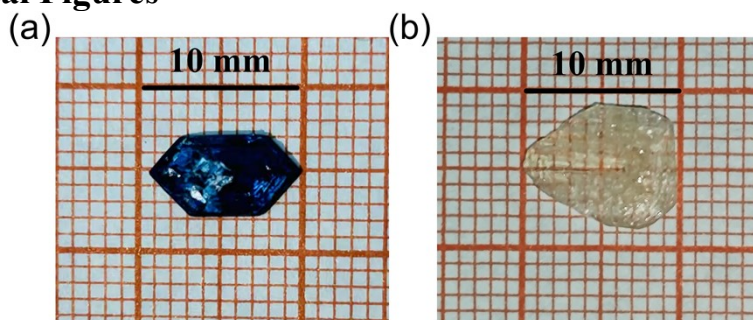


Figure S1. The macroscopic shape of the single crystal of crystal (a) DFCBC and (b) DFCBZ.

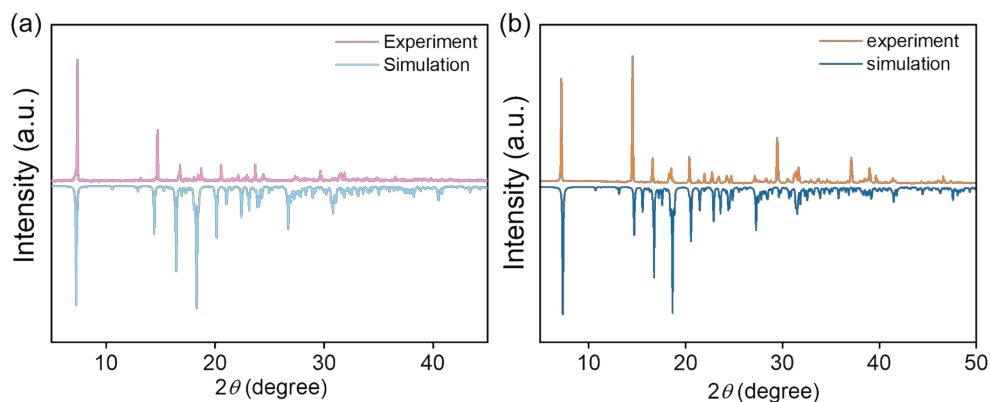


Figure S2. PXRD patterns of compound (a) DFCBC and (b) DFCBZ.

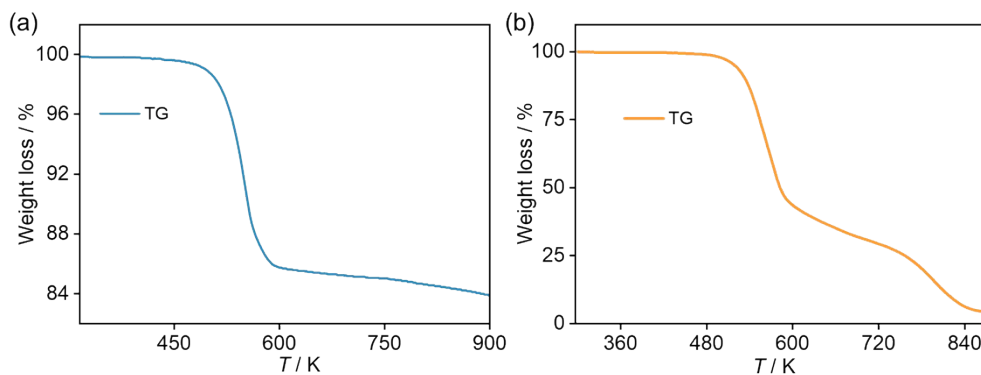


Figure S3. The thermogravimetric (TG) curve of compound (a) DFCBC and (b) DFCBZ.

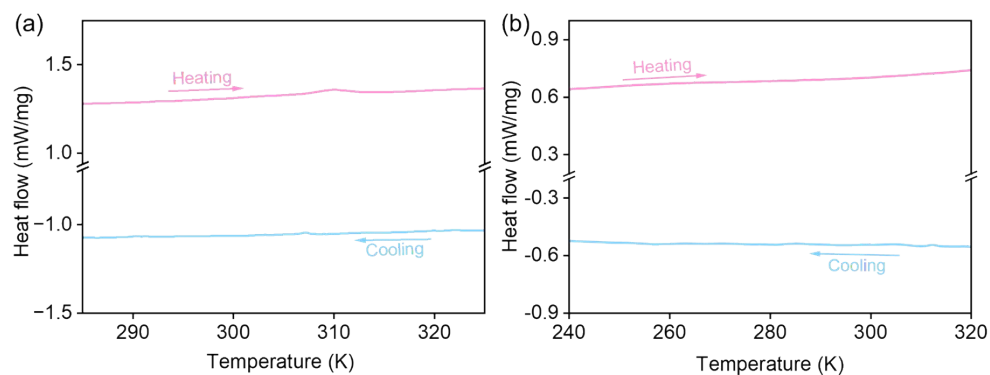


Figure S4. (a) DSC curves of CBC at 285–325 K. (b) DSC curves of CBZ at 240–320 K.

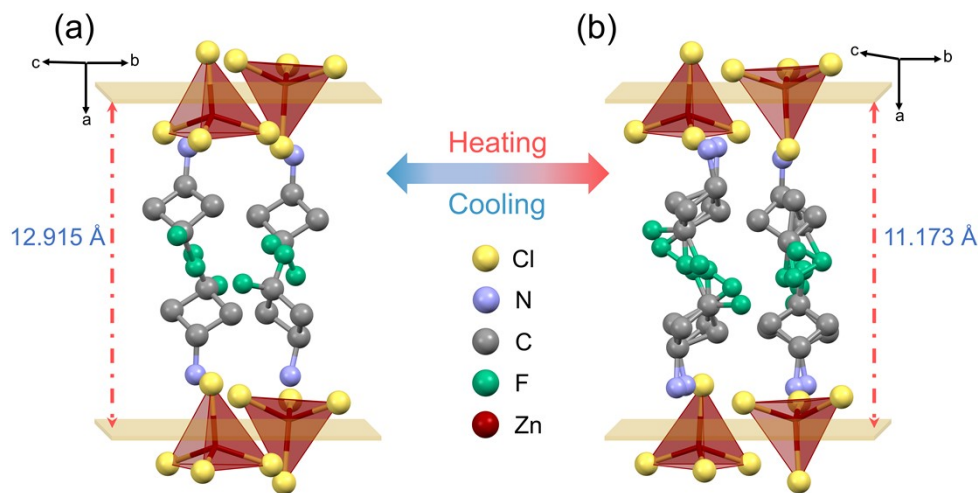


Figure S5. Perovskite structure of DFCBZ at (a) LTP and (b) HTP.

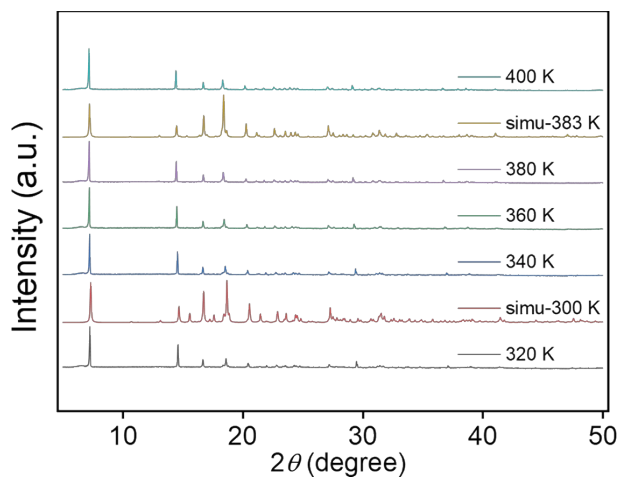


Figure S6. Comparison of simulated and experimental variable-temperature PXRD patterns of DFCBC.

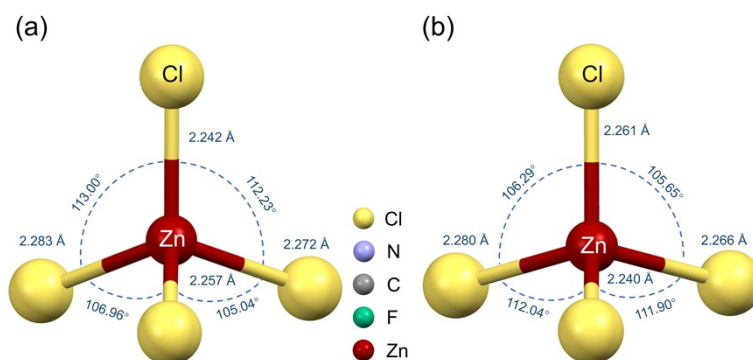


Figure S7. Zn-Cl bond length and Cl-Zn-Cl bond angle in DFCBZ in (a) LTP and (b) HTP.

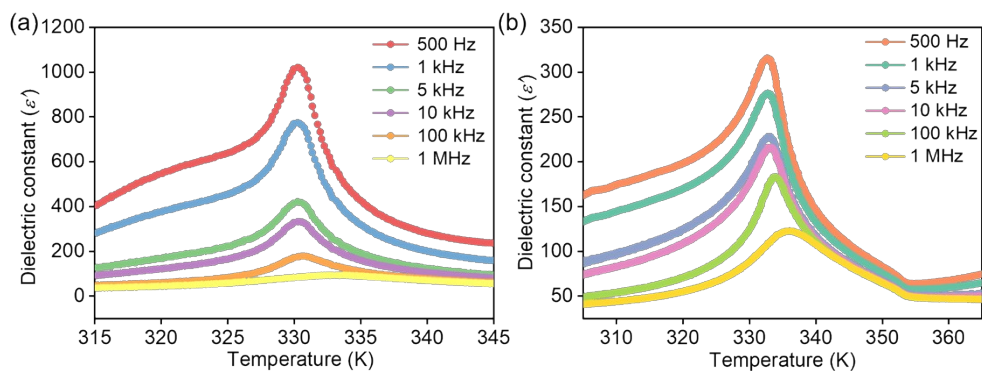


Figure S8. ϵ' and curves of the heating and cooling cycles of (a) DFCBC and (b) DFCBZ at different frequencies.

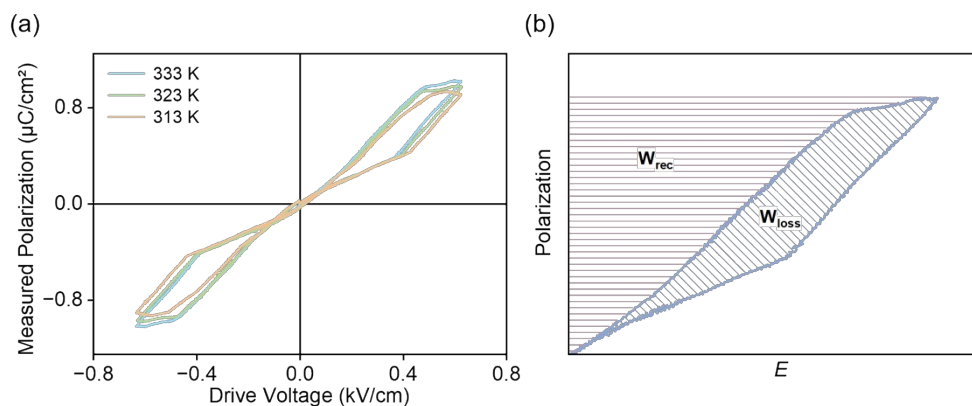


Figure S9. (a) Temperature dependence of P – E hysteresis loops of DFCBZ at 50 Hz. (b) Schematic diagram for the calculation of energy storage properties of antiferroelectric materials at 333 K.

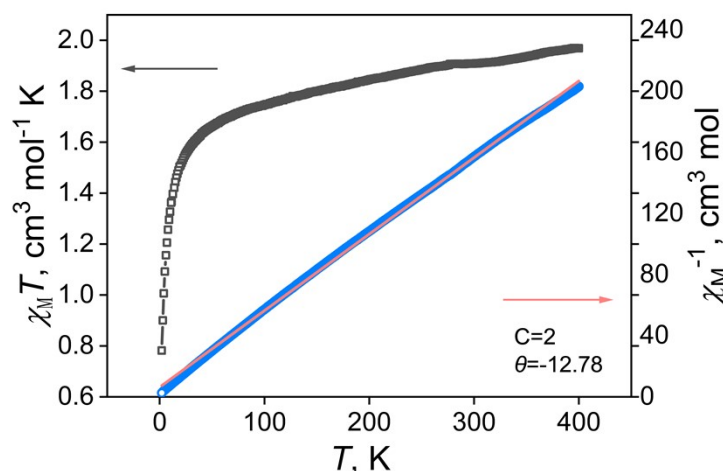


Figure S10. Temperature-dependent susceptibilities under a dc field of 1 kOe and Curie–Weiss fitted curves for DFCBC.

Supplemental Tables

Table S1. Crystal Data and Structure Refinement Details for DFCBC and CBC.

	DFCBC		CBC
T / K	300	383	300
Formula weight	414.96	416.96	344.99
Empirical formula	$C_8H_{16}Cl_4CoF_4N_2$	$C_8H_{14}Cl_4CoF_4N_2$	$C_8H_{17}Cl_4CoN_2$
Crystal system	monoclinic	monoclinic	monoclinic
Space group	$P2_1/n$	$P2_1/c$	$P\bar{1}$
$a / \text{\AA}$	11.9748(7)	12.2354(8)	7.2435(9)
$b / \text{\AA}$	11.3663(7)	11.5412(8)	10.7297(12)
$c / \text{\AA}$	24.1353(14)	11.9953(8)	11.8556(16)

$\alpha / ^\circ$	90	90	67.178(12)
$\beta / ^\circ$	91.858(5)	92.485(6)	75.090(12)
$\gamma / ^\circ$	90	90	81.855(10)
$V / \text{\AA}^3$	3283.3(3)	1692.3(2)	819.79(19)
Z	8	4	2
$D_{\text{calc}} / \text{g}\cdot\text{cm}^{-3}$	1.687	1.637	1.398
μ / mm^{-1}	1.722	1.671	1.675
$F(000)$	1696.0	836.0	354.0
$2\theta \text{ range} / ^\circ$	3.848–50.054	4.854–61.87	4.124–50.052
Reflns collected	21028	12154	8028
Independent reflns (R_{int})	55815 (0.0535)	4267 (0.0319)	2898 (0.0803)
No. of parameters	347	248	138
$R_1^{[\text{a}]}, wR_2^{[\text{b}]} [I > 2\sigma(I)]$	0.0969, 0.3310	0.0484, 0.1295	0.0686, 0.1752
R_1, wR_2 [all data]	0.1280, 0.3539	0.0996, 0.1493	0.1442, 0.2101
GOF	1.190	1.008	1.014
$\Delta\rho^{[\text{c}]} / \text{e}\cdot\text{\AA}^{-3}$	2.56, –1.33	0.44, –0.31	0.64, –0.38
CCDC	2450180	2450181	2450182

^[a] $R_1 = \Sigma||F_o| - |F_c||/|F_o|$; ^[b] $wR_2 = [\Sigma w(F_o^2 - F_c^2)^2]/\Sigma w(F_o^2)^2]^{1/2}$; ^[c] maximum and minimum residual electron density.

Table S2. Crystal Data and Structure Refinement Details for DFCBZ and CBZ.

	DFCBZ		CBZ
T / K	300	373	300
Formula weight	423.42	423.42	331.29
Empirical formula	$\text{C}_8\text{H}_{16}\text{Cl}_4\text{F}_4\text{N}_2\text{Zn}$	$\text{C}_8\text{H}_{16}\text{Cl}_4\text{F}_4\text{N}_2\text{Zn}$	$\text{C}_8\text{Cl}_4\text{N}_2\text{Zn}$
Crystal system	monoclinic	monoclinic	monoclinic
Space group	$P2_1/n$	$P2_1/c$	$P\bar{1}$
$a / \text{\AA}$	11.9762(4)	12.2125(11)	7.2353(5)
$b / \text{\AA}$	11.3823(4)	11.5496(12)	10.7252(7)
$c / \text{\AA}$	24.1133(9)	12.0034(9)	11.8483(9)
$\alpha / ^\circ$	90	90	67.005(7)
$\beta / ^\circ$	91.908(3)	92.476(8)	75.112(6)
$\gamma / ^\circ$	90	90	81.985(6)
$V / \text{\AA}^3$	3285.2(2)	1691.5(3)	817.17(11)
Z	8	4	2
$D_{\text{calc}} / \text{g}\cdot\text{cm}^{-3}$	1.712	1.663	1.346

μ / mm^{-1}	2.172	2.109	2.130
$F(000)$	1696.0	848.0	320.0
$2\theta \text{ range} / ^\circ$	4.922–61.488	4.856–61.332	4.13–61.658
Reflns collected	24811	11572	11445
Independent reflns (R_{int})	10239 (0.029)	5238 (0.0267)	5137 (0.0447)
No. of parameters	347	258	136
$R_1^{[\text{a}]}, wR_2^{[\text{b}]} [I > 2\sigma(I)]$	0.0892, 0.2948	0.0616, 0.2085	0.0563, 0.1629
R_1, wR_2 [all data]	0.1120, 0.3104	0.0903, 0.2305	0.1151, 0.1884
GOF	1.023	1.060	0.971
$\Delta\rho^{[\text{c}]} / \text{e}\cdot\text{\AA}^{-3}$	2.80, –1.45	0.86, –0.82	0.72, –0.30
CCDC	2450183	2450184	2450185

^[\text{a}] $R_1 = \Sigma||F_o| - |F_c||/|F_o|$; ^[\text{b}] $wR_2 = [\Sigma w(F_o^2 - F_c^2)^2]/\Sigma w(F_o^2)^2]^{1/2}$; ^[\text{c}] maximum and minimum residual electron density.

Table S3. Selected bond lengths [\AA] for DFCBC at 300 and 383 K.

DFCBC-300 K			
Co1–Cl1	2.256 (3)	Co1–Cl6	2.286 (3)
Co1–Cl2	2.266 (3)	Co1–Cl7	2.252 (3)
Co2–Cl4	2.263 (3)	Co2–Cl8	2.287 (3)
Co2–Cl5	2.272 (3)	Co2–Cl3	2.253 (3)
DFCBC-383 K			
Co1–Cl1	2.2498 (12)	Co1–Cl2	2.2593 (13)
Co1–Cl3	2.2640 (13)	Co1–Cl4	2.2786 (13)

Table S4. Selected bond lengths [\AA] for DFCBZ at 300 and 373 K.

DFCBZ-300 K			
Zn1–Cl1	2.242 (2)	Zn2–Cl5	2.272 (2)
Zn1–Cl2	2.2582 (18)	Zn2–Cl6	2.2418 (19)
Zn1–Cl3	2.272 (2)	Zn2–Cl7	2.2571 (18)
Zn1–Cl4	2.287 (2)	Zn2–Cl8	2.283 (2)
DFCBZ-373 K			

Zn1–Cl1	2.2402 (13)	Zn1–Cl3	2.2613 (14)
Zn1–Cl2	2.2662 (14)	Zn1–Cl4	2.2799 (15)

Table S5. Bond lengths [Å] of the hydrogen bond at 300 K of DFCBC.

<i>D–H···A</i>	<i>D–H</i>	<i>H···A</i>	<i>D···A</i>	<i>D–H···A</i>
N1–H1A···Cl6	0.89	2.35	3.239(8)	173
N1–H1B···Cl5	0.89	2.47	3.226(9)	144
N1–H1C···Cl1	0.89	2.56	3.286(8)	139
N1–H1C···Cl2	0.89	2.73	3.420(9)	135
N2–H2A···Cl8	0.89	2.69	3.455(9)	145
N2–H2B···Cl4	0.89	2.33	3.203(8)	167
N2–H2C···Cl6	0.89	2.80	3.583(9)	148
N3–H3A···Cl6	0.89	2.59	3.426(10)	156
N3–H3B···Cl1	0.89	2.30	3.155(10)	161
N3–H3C···Cl4	0.89	2.82	3.335(9)	118
N4–H4A···Cl2	0.89	2.40	3.225(8)	153
N4–H4B···Cl4	0.89	2.73	3.259(8)	119
N4–H4B···Cl5	0.89	2.53	3.346(8)	153
N4–H4C···Cl8	0.89	2.40	3.266(8)	164

Table S6. Bond lengths [Å] of the hydrogen bond at 383 K of DFCBC.

<i>D–H···A</i>	<i>D–H</i>	<i>H···A</i>	<i>D···A</i>	<i>D–H···A</i>
N1–H1A···Cl3	0.89	2.41	3.243(4)	157
N1–H1B···Cl2	0.89	2.81	3.321(4)	118
N1–H1B···Cl3	0.89	2.55	3.389(4)	157
N1–H1C···Cl4	0.89	2.40	3.250(4)	161
N2–H2A···Cl4	0.89	2.67	3.468(4)	150
N2–H2B···Cl2	0.89	2.32	3.199(4)	169

Table S7. Bond lengths [\AA] of the hydrogen bond at 300 K of DFCBZ.

$D-H\cdots A$	$D-H$	$H\cdots A$	$D\cdots A$	$D-H\cdots A$
N1-H1A \cdots C14	0.89	2.61	3.423(8)	152
N1-H1B \cdots C17	0.89	2.34	3.330(8)	120
N1-H1C \cdots C12	0.89	2.34	3.172(7)	156
N2-H2A \cdots C18	0.89	2.69	3.439(7)	142
N2-H2B \cdots C14	0.89	2.79	3.606(7)	152
N2-H2C \cdots C17	0.89	2.33	3.194(7)	163
N3-H3A \cdots C14	0.89	2.36	3.235(7)	168
N3-H3B \cdots C12	0.89	2.67	3.298(7)	129
N3-H3B \cdots C13	0.89	2.64	3.416(6)	146
N3-H3C \cdots C15	0.89	2.42	3.231(6)	152
N4-H4A \cdots C13	0.89	2.42	3.232(6)	151
N4-H4B \cdots C18	0.89	2.38	3.255(7)	168
N4-H4C \cdots C15	0.89	2.55	3.350(6)	150
N4-H4C \cdots C17	0.89	2.71	3.276(7)	123

Table S8. Bond lengths [\AA] of the hydrogen bond at 373 K of DFCBZ.

$D-H\cdots A$	$D-H$	$H\cdots A$	$D\cdots A$	$D-H\cdots A$
N1-H1A \cdots C12	0.89	2.47	3.245(4)	146
N1-H1B \cdots C14	0.89	2.37	3.257(5)	179
N1-H1C \cdots C12	0.89	2.66	3.385(4)	139
N1-H1C \cdots C13	0.89	2.65	3.318(5)	133
N2-H2A \cdots C14	0.89	2.79	3.551(14)	144
N2-H2B \cdots C14	0.89	2.80	3.575(12)	146
N2-H2C \cdots C13	0.89	2.35	3.227(16)	169